Available online at www.sciencedirect.com

ScienceDirect

journal homepage: www.elsevier.com/locate/he

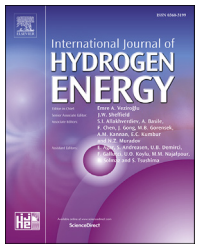

Coke minimization via SiC formation in dry reforming of methane conducted in the presence of Ni-based core–shell microsphere catalysts

Gamze Gunduz Meric [a], Huseyin Arbag [b], Levent Degirmenci [a,*]

[a] Department of Chemical and Process Engineering, Bilecik Seyh Edebali University, Bilecik 11210, Turkey
[b] Department of Chemical Engineering, Gazi University, Ankara 06570, Turkey

ARTICLE INFO

Article history:
Received 28 March 2017
Received in revised form
15 May 2017
Accepted 16 May 2017
Available online 7 June 2017

Keywords:
Sol–gel microencapsulation
Dry reforming of methane
Methane cracking
Boudard
Silicon carbide

ABSTRACT

Mesoporous Ni/Si microsphere catalysts were synthesized with a modified sol–gel microencapsulation method and their activity was tested in dry reforming of methane (DRM) reaction. Results indicated comparable conversion values and H_2/CO ratios with other catalysts reported in literature. Activity loss of 5% determined with time on stream analysis of 5% Ni/Si catalyst revealed that sustainable production could have been possible in the presence of these catalysts. Coke deposition which was frequently stated as the reason of activity loss was not observed with Ni/Si microsphere catalysts. Taking into account the impossibility of eliminating methane cracking and Boudard reaction during DRM, we should come up with an explanation of the absence of coke. This explanation was provided by silicon carbide (SiC) formation which consumed the coke deposited on the catalyst. Characterization analyses conducted at spent catalysts validated both the absence of coke and formation of SiC during DRM.

Introduction

Shale gas recovery using current technology is important as its amount worldwide constitutes a comparable portion with natural gas [1]. The majority of shale gas is methane, a greenhouse gas which can be evaluated in the production of synthesis gas when used with carbon dioxide, also a greenhouse gas. Recovery of shale and production of synthesis gas from greenhouse gases are two goals that could be achieved by dry reforming of methane (DRM). The produced syngas with a H_2/CO ratio of 1 can be used as feedstock in a variety of reactions such as Fischer–Tropsch synthesis, methanol and dimethyl ether production [2–6]. Synthesis gas is produced based on the following reaction:

$$CH_4 + CO_2 \leftrightarrow 2CO + 2H_2 \quad \Delta H^{\circ}_{298} = 247 \text{ kJ mol}^{-1} \tag{1}$$

Side reactions such as reverse water gas shift reaction (RWGS) (Eq. (2)), methanation reaction (Eq. (3)) and steam reforming of methane (Eq. (4)) also occur simultaneously.

$$CO_2 + H_2 \leftrightarrow CO + H_2O \quad \Delta H^{\circ}_{298} = 41 \text{ kJ mol}^{-1} \tag{2}$$

$$CO_2 + 4H_2 \leftrightarrow CH_4 + 2H_2O \quad \Delta H^{\circ}_{298} = -165 \text{ kJ mol}^{-1} \tag{3}$$

$$CH_4 + H_2O \leftrightarrow CO + 3H_2 \quad \Delta H^{\circ}_{298} = 206 \text{ kJ mol}^{-1} \tag{4}$$

* Corresponding author. Fax: +90 228 2141222.
E-mail address: levent.degirmenci@bilecik.edu.tr (L. Degirmenci).
http://dx.doi.org/10.1016/j.ijhydene.2017.05.121

The ratio of H_2/CO obtained by DRM is always below 1due to the effect of RWGS. Coke deposition is another principal factor preventing to reach the desired ratio. Coke deposition, in long term use also hinders catalytic activity. Coke deposition occurs via CH_4 cracking (Eq. (5)) and Boudouard reactions (Eq. (6)) [6].

$$CH_4 \rightarrow C + 2H_2 \quad \Delta H^{\circ}_{298} = 75 \text{ kJ mol}^{-1} \tag{5}$$

$$2CO \rightarrow C + CO_2 \quad \Delta H^{\circ}_{298} = -173 \text{ kJ mol}^{-1} \tag{6}$$

It is possible to increase H_2/CO ratio to a certain level by utilizing active catalysts. However, coke formation rather than efficiency is the problem in these reactions. In order to maintain sustainable production, the catalyst used for DRM must both be cost effective and resilient to coke formation [7–9]. The noble metal catalysts (Rh, Ru, Pt, Pd and Ir) have good catalytic activity and carbon resistance [10]. However, their use are limited due to high costs in large scale applications [11]. As an alternative, Fe, Co and Ni based catalysts have widely been investigated for their potential in industrial utilization. These catalysts have lower cost and have good activity with high selectivity in reactions [12–15]. The main problem with Ni-based catalysts is their low coking resistance [16]. Sintering of Ni during reaction must be prevented in order to eliminate coke formation and studies revealed that coke formation of Ni could have been decreased by coating the active material with a silica shell [9,17,18]. Silica (SiO_2) has long been used as a carrier in catalyst synthesis due to its high surface area and metal surface dispersion [19–23].

Recent studies on dry reforming of methane have shown that carbon deposition and sintering resulted in the loss of catalytic activity [24]. Core–shell structures, on the other hand can provide a shelter for Ni particles protecting them from sintering and hence this confinement medium helps elimination of coke formation [9,19,21,23,25,26]. Various findings for the explanation of coke elimination were reported in literature. In the work of Majeswki et al., a strong interaction between nickel and the silica support in the form of nickel phyllosilicate was stated as the reason of high activity and stability of the catalysts towards methane steam reforming [19]. Ding et al. referred to the effect of surface state of the active nickel metal and stated that coke formation had been enhanced with increasing amount of NiO inside silica structure [21]. Studies showed the compatibility of Nickel and silica in catalyst synthesis. In a study conducted by Kang et al. [27]. immobilization of Ni-chelating polyethyleneimine complexes in mesoporous silica was conducted. The activity of the synthesized catalyst tested through DRM indicated stable activity at 750 °C for 4 h with much smaller carbon deposition compared to bare Ni containing mesoporous silica synthesized without polyethyleneimine [27]. SBA 15, a well known silica based mesoporous material is also used as catalyst support in Ni containing catalysts. 10% Ni/SBA-15 catalyst was utilized for DRM in the work of Omoregbe et al. [28]. Reaction experiments were conducted at atmospheric pressure with varying CH_4/CO_2 volume ratios at 923 and 1023 K. Results indicated a stable activity for 4 h of reaction, a decrease in activity was observed at 923 K due to coke formation. Conversions values of CH_4 and CO_2 were determined as 91 and 94% for the reaction conducted at 1023 K and 20 kPa partial pressures [28]. Synthesis procedures applied in catalyst synthesis are also important in obtaining stable activity with Ni containing catalysts. In a work conducted by Zhang et al. [29], Catalysts were synthesized by impregnation onto SBA-15. The active material used in synthesis is the chelate of Ni metal which was obtained using ethylene diamine, citric acid and acetic acid. It was reported that high viscosity of these chelating agents had a positive effect on Ni dispersion and the activity in DRM was also higher in the presence of these catalysts compared with the ones prepared by conventional method [29]. As previously mentioned, coke deposition is inevitable in Ni based catalysts and the use of Ni with other metals was among the solutions being investigated to decrease coke formation and enhance catalytic activity. Synthesis of Ni based mesoporous silica catalysts by sol–gel addition of Neodymium (Nd) was utilized in DRM and the effect of Nd on catalyst activity and stability was determined for varying Nd/Si ratios in the catalyst. Results indicated an enhanced activity for the first 12 h of reaction in the presence of Nd inside the catalyst. This result was attributed to modified interaction of Ni and the support by Nd addition [30]. A non-conventional synthesis of Ni/SBA-15 catalysts was conducted by ascorbic acid addition as reducing agent and the applied synthesis was compared to conventional methods in a study conducted by Galvez et al. [31]. Results indicated an improved selectivity and hindered deactivation. Carbon deposition in the presence of ascorbic acid was stated to be in favour of amorphous carbon with growth mostly on the external surface of the catalyst [31].

In the present study, dry reforming of methane in the presence of Ni/Si microsphere catalyst was investigated with varying Ni amounts inside the shell structure. SiC formation during DRM was observed and its contribution in the elimination of coke formation was illustrated for the first time based on our knowledge. The synthesized catalysts have excellent resistance towards coke formation and their activity and selectivity were comparable to those reported in literature [1,5,23,26].

Experimental

Catalysts preparation

Ni based silica microspheres were prepared by modification of sol–gel microencapsulation method reported in literature [32]. 0.5 g hexadecyl cetyl trimethyl ammonium bromide (CTAB, Merck) and varying amounts of $Ni(NO_3)_2 \cdot 6H_2O$ (Merck) were dispersed in 20 ml deionized water by ultra-sonication for 15 min. The resulting solution was homogenized in a mixture of 50 ml ethanol and 10 ml 25 wt.% ammonia solution. 5 ml of TEOS (tetraethylorthosilicate, Merck) was added dropwise to resulting solution. The amount of Nickel inside the microsphere was determined based on the weight of Ni in its salt to the amount of silicium inside TEOS. Ni/Si amount in microspheres were determined as 1.25, 5 and 10%. After stirring at room temperature for 6 h, the product was washed with ethanol and deionized water for 3 times and dried at room temperature for 24 h. The catalysts were calcined at

Table 1 – Textural and physical properties of Ni/Si microsphere catalysts.

Sample	BET surface area, m^2/g	Pore size, nm	Pore volume, cm^3/g
1.25% Ni	419.2	2.4	0.18
5% Ni	434.3	2.3	0.23
10% Ni	450.2	2.3	0.30

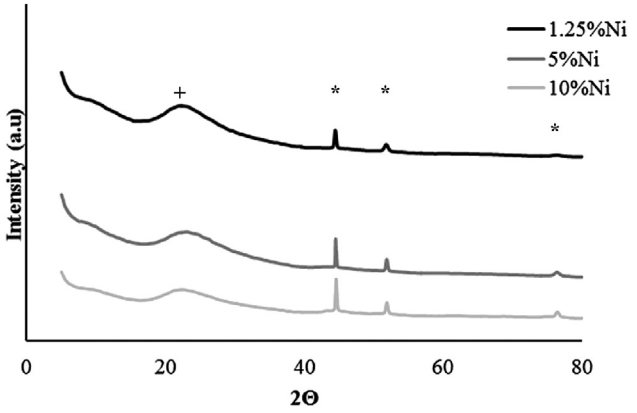

Fig. 1 – X-ray diffraction patterns of the Ni core–shell catalysts (+: Si; *: Ni).

750 °C for 6 h at the heating rate of 1 °C/min. Finally, NiO containing microsphere catalysts were reduced to Ni form at 750 °C in a flow of hydrogen for 3 h.

Characterization of microsphere catalysts

Nitrogen adsorption–desorption, X-ray diffraction (XRD), Scanning electron microscopy (SEM), inductively coupled plasma-mass spectroscopy (ICP-MS) techniques were used in characterization of synthesized catalysts. The results obtained from these analyses were evaluated in accordance with XRD, SEM, thermal analysis (TGA), attenuated total reflectance Fourier transform infrared spectroscopy (ATR-FT-IR) and Raman spectroscopy results of the catalysts recovered after reaction. Results were interpreted to explain the state of molecular structure, coke and/or SiC formation after reaction. The X-ray diffraction (XRD) patterns were obtained by a Panalytical Empyrean instrument ($\lambda = 1.5418$ Å) at 200 kV and 50 mA in the range of 2Θ value between 5° and 80° with a speed of 10° min^{-1}. BET surface area, pore volume and pore size distributions of the catalysts were measured by the nitrogen adsorption–desorption method, using a Micromeritics Asap 2020 instrument. Samples were pretreated at 300 °C for 4 h prior to BET analysis. The surface morphology of microspheres was determined using a SEM, Zeiss Supra 40 V device. Metal loading of Ni was determined by ICP-MS using a Perkin Elmer DRC II device. Thermogravimetric analyses in the presence of air were conducted with Hitachi Exstar SII TG/DTA 7300 device in a temperature range of 25–900 °C at a rate of 10 °C/min. Raman spectroscopy was performed on a Bruker FRA 106/S Raman instrument using a $\lambda = 532$ nm Nd-YAG laser. ATR-FT-IR studies were performed using a Cary 630 Fourier transform

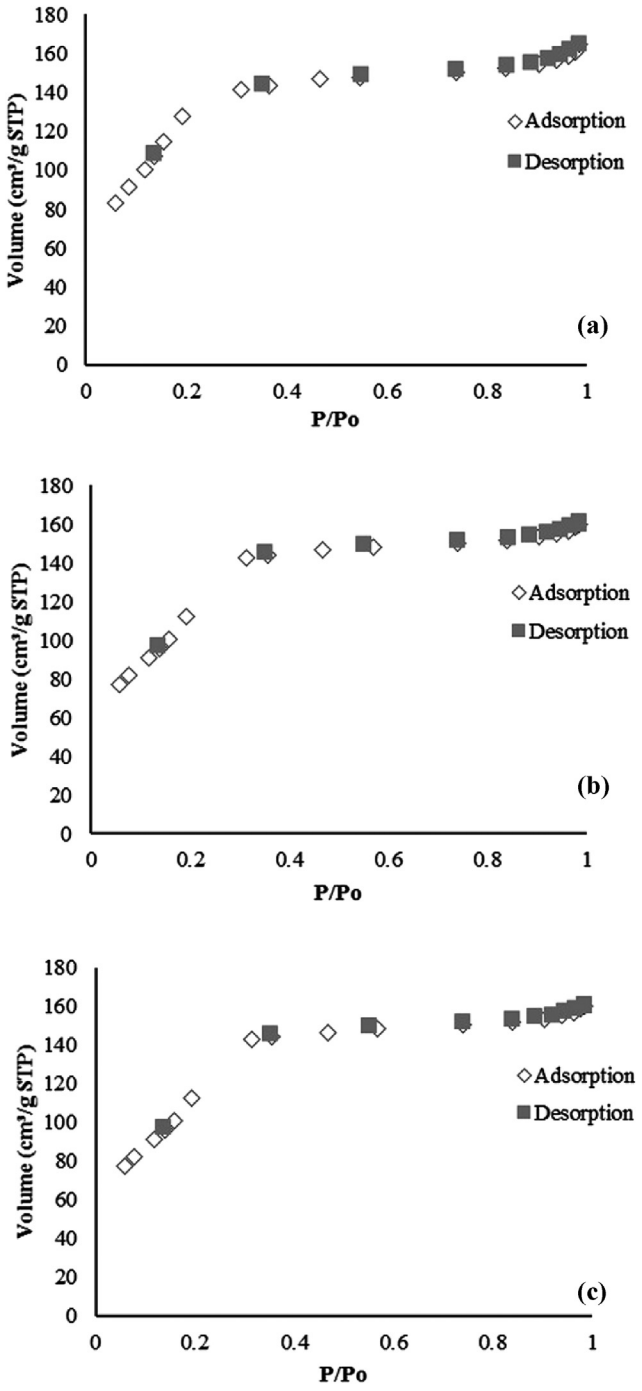

Fig. 2 – N_2 isotherms of Ni/Si microsphere catalysts (a) 1.25% Ni (b) 5% Ni and (c) 10% Ni.

Table 2 – ICP-MS results of the catalysts.

Sample	Ni content (%)	
	Synthesis solution	ICP-MS
1.25 Ni	1.25	1.23
5 Ni	5	3.20
10 Ni	10	5.43

infrared spectrometer, equipped with a single reflection diamond attenuated total reflectance (ATR) accessory.

Catalytic reactions

DRM reactions were carried out in a fixed bed reactor fitted inside a quartz tube (inner diameter of 6 mm). The catalysts, reduced with a flow of hydrogen for 3 h at 750 °C, were loaded in the quartz tube reactor. A total of 0.1 g catalyst was used in reaction experiments. A mixture of CH_4, CO_2 and Ar with volume ratio of 1 (CH_4:CO_2:Ar = 1:1:1) was fed with 20 ml/min. Experiments were performed at a space velocity of 36,000 ml/(g_{cat} h). The reactant and product stream leaving the quartz tube were analyzed on-line by gas chromatography (Perkin Elmer Autosystem XL), which was equipped with a thermal conductivity detector and a Carbosphere column. The catalytic tests were conducted at 750 °C for 3 h at atmospheric pressure. The experiments were repeated in identical conditions and the average data values were illustrated in the results. The equations used in calculating the conversions of CH_4 and CO_2 (Eq. (7) and (8)) and the selectivities of CO and H_2 (Eq. (9) and (10)) determined with respect to converted CH_4 were given below [33]:

$$CH_4 \text{conversion} : X_{CH_4} = (CH_{4\,in} - CH_{4\,out})/CH_{4\,in} \quad (7)$$

$$CO_2 \text{conversion} : X_{CO_2} = (CO_{2\,in} - CO_{2\,out})/CO_{2\,in} \quad (8)$$

$$H_2 \text{ selectivity} : S_{H_2(CH_4)} = H_{2\,out}/(CH_{4\,in} - CH_{4\,out}) \quad (9)$$

$$CO \text{ selectivity} : S_{CO(CH_4)} = CO_{out}/(CH_{4\,in} - CH_{4\,out}) \quad (10)$$

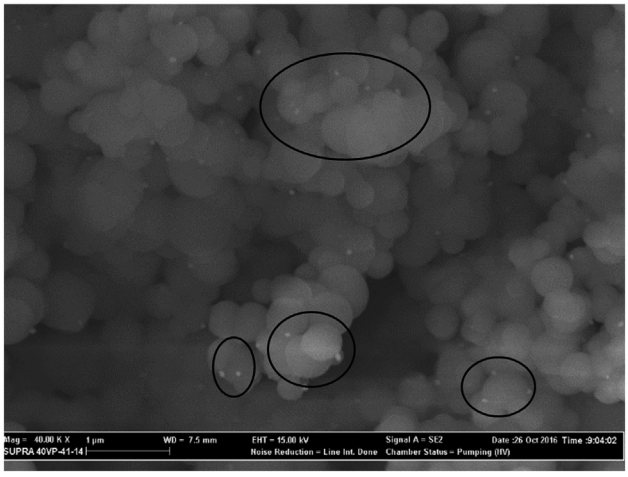

Fig. 4 – SEM images of crushed microsphere catalyst and uncoated Ni particles.

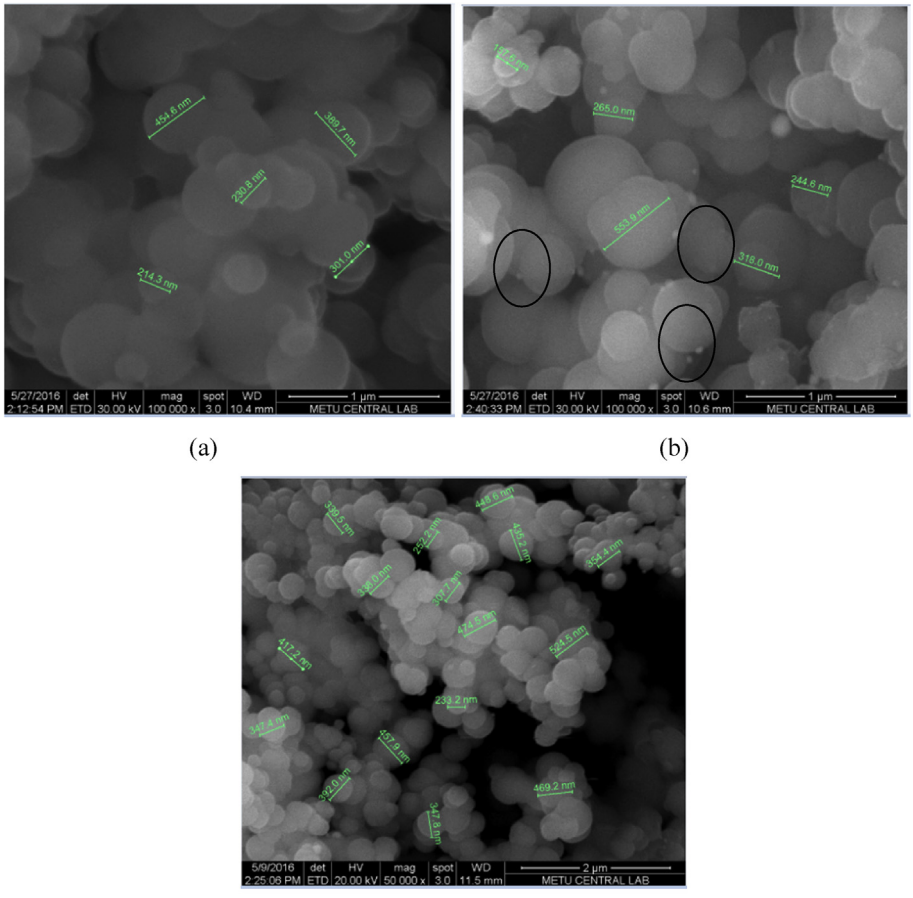

(a) (b) (c)

Fig. 3 – SEM images of the microsphere catalysts (a) 1.25% Ni (b) 5% Ni (c) 10% Ni.

Results and discussions

Characterization of synthesized catalysts

Textural and physical properties of Ni/Si microsphere catalysts synthesized with varying Ni amounts were illustrated in Table 1. An increase in surface area and pore volume of the catalysts with increasing Ni amount were observed as seen from the table. The increase was due to the porous structure of nickel and the increase of porosity emanated from nickel presence resulted in the increase of surface area and pore volume [19].

XRD patterns of Ni containing microsphere catalysts prepared with different amounts of Ni loading are given in Fig. 1. The peaks observed at 2θ values of 44.6, 51.9 and 76.4° corresponded to (111), (200) and (220) reflections of Ni metal [34]. The broad peak obtained at 23.5° corresponded to amorphous silica [35]. The intensity of 5% Ni catalyst was higher than 1.25% catalyst but close to 10% Ni catalyst implying some loss of active material be observed with loading amounts higher than 5% (Fig. 1). N_2 adsorption–desorption isotherms of catalysts were Type IV according to IUPAC classification which indicated the formation of mesoporous structure with narrow pore size distribution [9,36,37] (see Fig. 2).

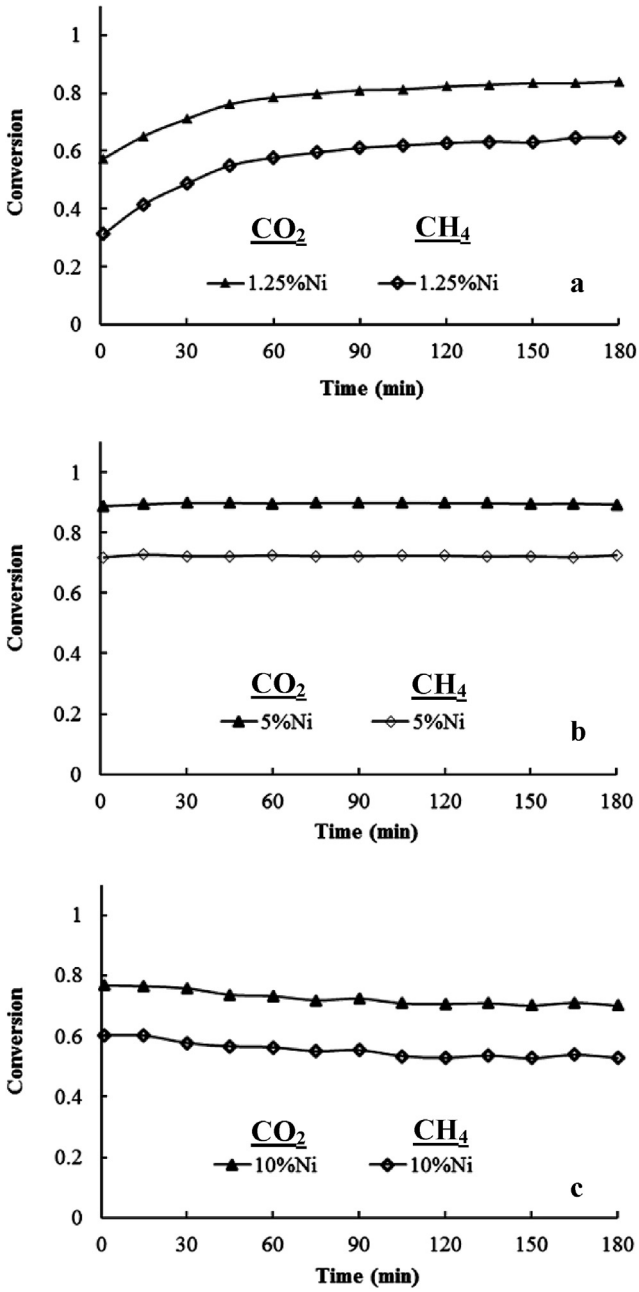

Fig. 5 – CH_4 and CO_2 conversions obtained in te presence of (a) 1.25% Ni (b) 5% Ni and (c) 10% Ni catalysts (Reaction temperature: 750 °C, CH_4/CO_2/Ar: 1/1/1).

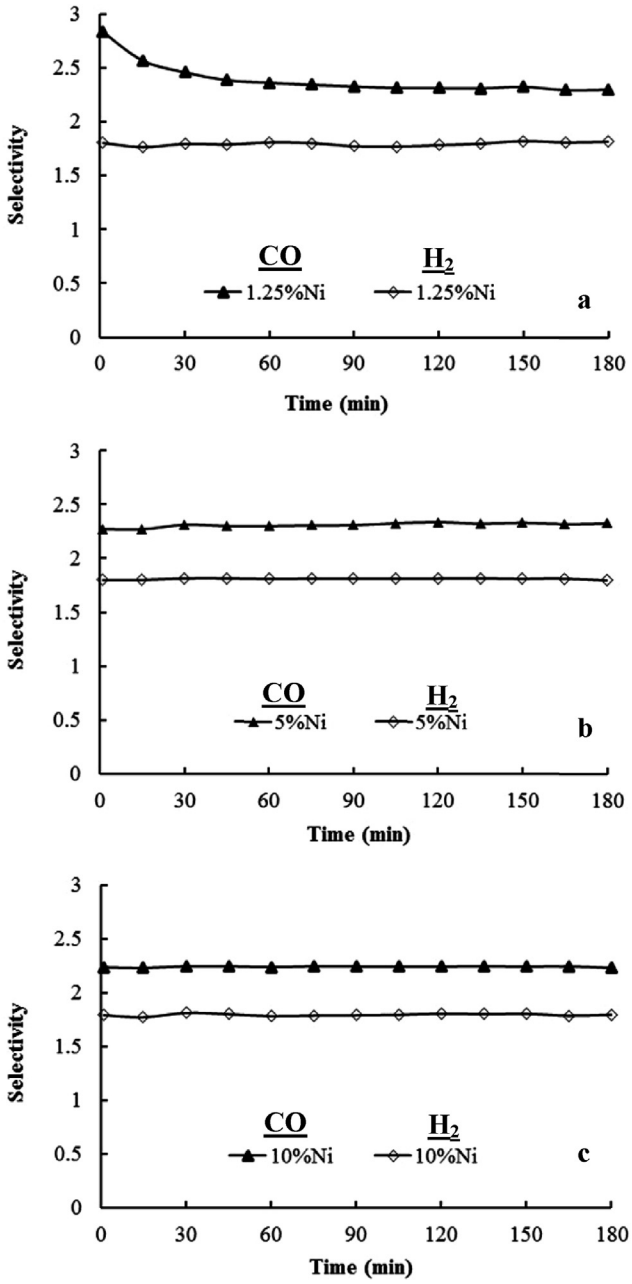

Fig. 6 – H_2 and CO selectivities over (a) 1.25% Ni (b) 5% Ni and (c) 10% Ni. Reaction temperature: 750 °C, CH_4/CO_2/Ar: 1/1/1.

The amount of Ni loss from the catalyst was determined by ICP-MS analyses conducted on the catalysts. Results, as shown in Table 2 indicated a significant loss of active material for the catalyst synthesized with 10% Ni loading.

Fig. 3 displays the SEM images of the catalysts. As previously mentioned, microsphere formation has occurred as a result of Ni encapsulation by a silica shell and the images validated formation of microsphere. However, formation of small particles on microsphere surface has also been observed indicating the presence of uncoated Ni particles (shown by black circle in Fig.). As a matter of fact it is hard to say whether these particles are Ni, based on the results presented. In order to validate the presence of uncoated Ni, microspheres were corroded and SEM images of these microspheres were also obtained. As seen from, Fig. 4, the amount of small particles has increased as a result of corrosion which was due to the increase of the amount of Ni particles on the surface or near-surface layer.

Catalytic performance of the catalysts in dry reforming of methane

DRM reactions were conducted in the presence of Ni loaded microspheres at 750 °C. Catalysts were reduced in a flow of hydrogen at 750 °C for three hours, prior to experiments. A mixed stream of CH_4, CO_2 and Ar with volume ratio of 1 (CH_4:CO_2:Ar = 1:1:1) was introduced to a fixed bed reactor containing 0.1 g catalyst. Results were illustrated in terms of methane, carbon dioxide conversions (Fig. 5). Hydrogen and carbon monoxide selectivities (Fig. 6) were calculated by interpretation of experimental results. CH_4 conversions at the end of 3 h were determined as 0.65, 0.73 and 0.53 for 1.25, 5 and 10% Ni catalysts. Higher CO_2 conversions (0.84, 0.89, and 0.70, respectively) were obtained due to RWGS, as expected. Conversion values were compared with equilibrium conversions (Supplementary file Fig. 1) obtained via Gaseq Chemical Equilibrium Programme. Results indicated that equilibrium had been approached in terms of CO_2 conversion in the presence of 5% Ni catalyst. This catalyst was the most stable one and showed no change in its performance within the investigated reaction time.

H_2 and CO selectivities were calculated based on the moles of CH_4 converted. Contribution of RWGS reaction could better be followed by comparing selectivity values of H_2 and CO which should be 2 in ideal case. However, CO selectivity higher than 2 and H_2 selectivity lower than 2 were obtained indicating the effect of RWGS reaction during DRM. CO selectivity values were 2.30, 2.23, 2.33 for 1.25, 5 and 10% Ni microsphere catalysts, respectively. H_2 selectivities were 1.80 for all of the catalysts.

The catalyst synthesized in our study has shown good activity for DRM reaction. The H_2/CO ratio which was another parameter to assess the efficiency of reaction was also close to 1. However, a comparison with literature must be made in order to better visualize the extent of its activity and efficiency. Literature survey showed a great number of studies regarding to DRM reaction. These studies were conducted in the presence of a variety of catalysts with varying experimental conditions and selected studies were summarized in Table 3. It was clearly seen from the table that synthesized catalyst had been among the ones with highest activity and efficiency.

It is obvious from reaction experiments and characterization analyses that 5% Ni/Si microsphere catalyst had the highest activity and stability among those synthesized by varying Ni amounts. Consequently, this catalyst was selected to determine its time on stream performance with 18 h

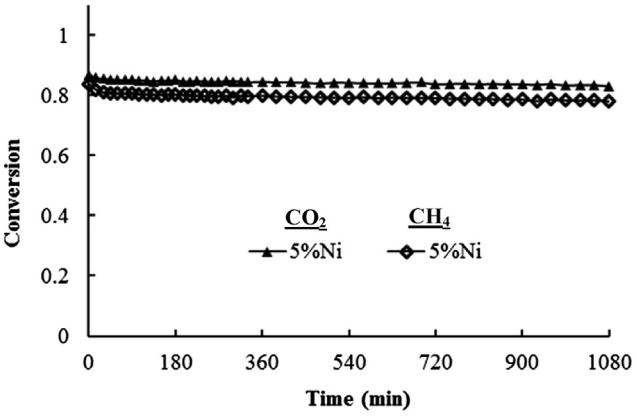

Fig. 7 – Time on stream performance of 5% Ni/Si microsphere catalyst Reaction temperature: 750 °C, CH_4/CO_2/Ar: 1/1/1.

Table 3 – Literature comparison of the synthesized catalyst in similar experimental conditions.

Researcher	Catalyst	Reaction conditions	CH_4 conversion	H_2/CO ratio
[1]	Ni/Al_2O_3	750 °C, 1 atm CH_4/CO_2: 1/1 WHSV: 132,000 ml/(gcat h)	0.72	0.68
[5]	$Ni@SiO_2$	750 °C, 1 atm CH_4/CO_2: 1/1 WHSV: 18,000 ml/(gcat h)	0.85–0.90	0.91
[23]	$Ni@SiO_2$ yolk–shell	700 °C, 1 atm CH_4/CO_2: 1/1 WHSV: 12,000 ml/(gcat h)	0.61	0.6
[26]	NiCe@m-SiO_2 yolk–shell	750 °C, 1 atm CH_4/CO_2: 1/1 WHSV: NA*	0.90	NA
This work	5% Ni/SiO_2 microsphere	750 °C, 1 atm CH_4/CO_2: 1/1 WHSV: 36,000 ml/(gcat h)	0.73	0.80

reaction test conducted at identical conditions (Fig. 7). Results indicated a 5% decrease of both CO_2 and CH_4 conversions. In other words, the catalyst could have been used without any significant loss of activity. H_2 and CO selectivities remained unchanged during reaction and H_2/CO ratio was obtained as 0.80 at the end of 18 h. This was among the most important results of the present study as it showed the possibility of a sustainable production in long-term production of syngas in the presence of microsphere catalysts.

Characterization of spent catalysts

XRD analysis with spent catalysts was conducted in order to examine the effect of reaction conditions on molecular structure of the catalyst. The peaks obtained from spent catalysts were the same with synthesized catalysts indicating no change of molecular structure. The peak value at $2\Theta = 26^\circ$ belonged to amorphous silica as previously stated (Fig. 8d). Elimination or at least mitigation of coke formation was aimed in almost all the works regarding DRM. Consequently, our primary intent was first to determine the presence of coke on spent catalysts and then its amount which could be achieved by SEM and TGA analyses. SEM images, as seen in Fig. 8, validated the presence of filamentous coke especially near uncoated Ni particles (shown in black circle).

TGA analysis on spent catalysts was conducted to determine the amount of coke formed during reaction (Fig. 9). However except for the region that belonged to vaporization of moisture, it was interesting to observe an increase on weight which should have been the exact opposite due to possible decomposition of coke via oxidation during TGA analysis. The first thing come to mind could be the oxidation of reduced Ni in the catalyst which has been reported in various temperature intervals in literature [38,39]. However, two regions of weight increase were determined in TGA analysis (Supplementary file Fig. 2) which could not be explained by the results obtained so far. The temperature of this second region of weight increase varied with increasing Ni amount in the microsphere. Total weight increase obtained from TGA analyses were determined as 1.61, 3.46 and 4.4% for 1.25, 5 and 10 Ni loadings, respectively. Considering that all of theoretically determined Ni was present inside the microsphere, the amount of weight added by NiO formation was still far below total weight increase which implied formation of compounds other than NiO. In our opinion this weight increase was emanated from oxidation of Si or SiC that might have been in catalyst structure. Oxidation of pure SiC occurred at 300 °C and oxidation of aniline added SiC occurred at 500 °C in the work of Kormanyos et al. [40]. Hence it will be fair to at least imply that SiC oxidation may contribute to the second region

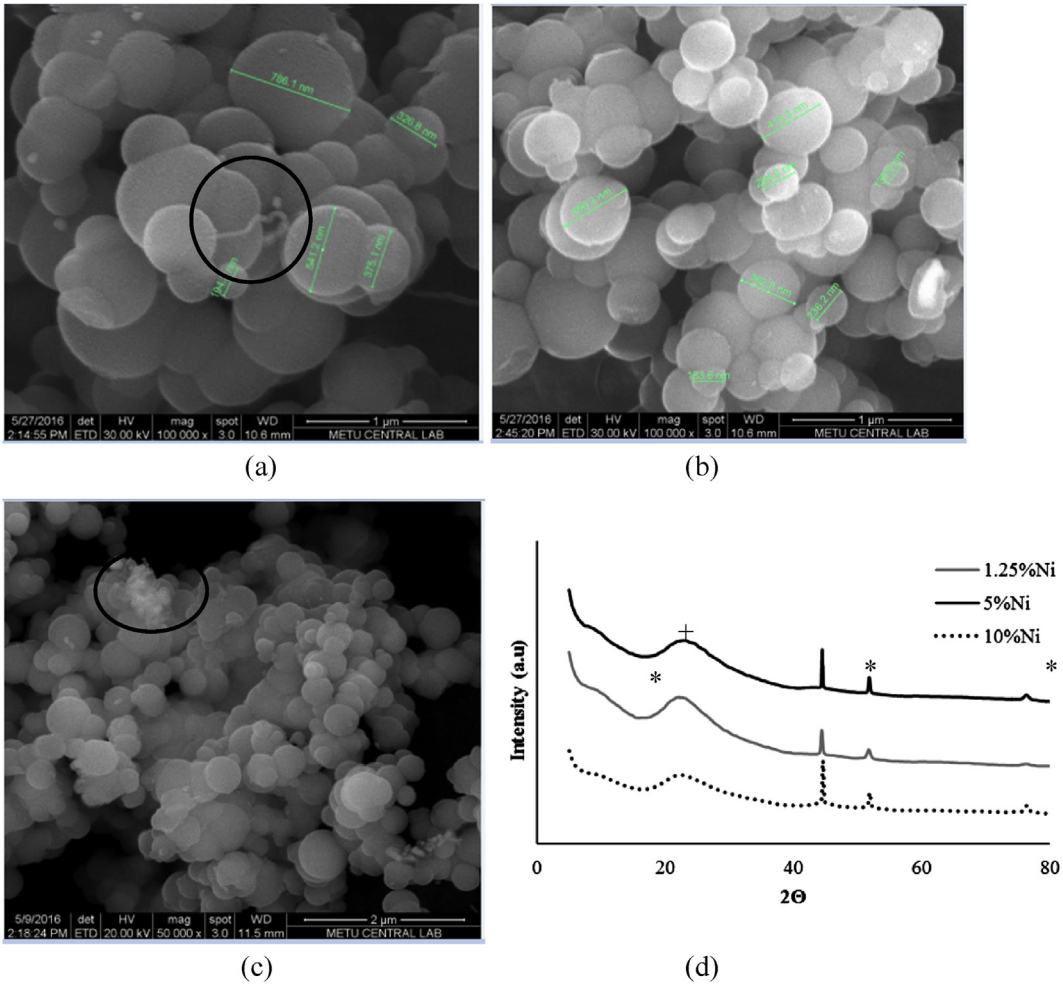

Fig. 8 – SEM images of a) 1.25% b) 5% c) 10% Ni/Si microsphere catalysts d) XRD patterns of spent catalysts (+: Si; *: Ni).

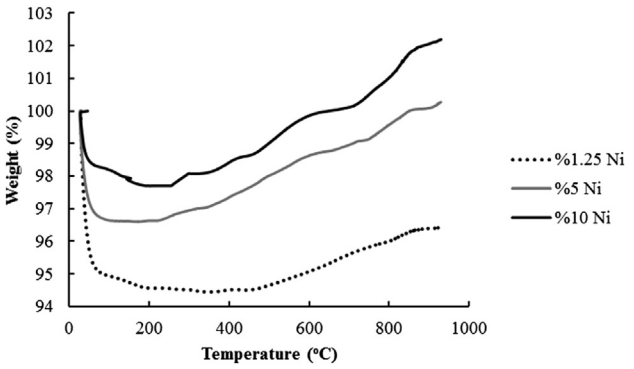

Fig. 9 – TGA profiles of spent catalysts obtained after 3 h reaction time at 750 °C (CH_4/CO_2/Ar: 1/1/1).

mentioned in TGA analyses. On the other hand, crystalline SiC was formed with the reaction between silica and petroleum coke at temperatures much higher than the reaction of DRM [41] and its formation must have been detected in XRD patterns. Literature survey revealed that the onset of crystalline SiC formation had been determined as 1000 K which was closer to our reaction temperature. Temperatures below 1000 K yielded amorphous SiC which could be the reason of its absence in XRD patterns (Fig. 8d) [42]. Having said that it could still be possible to detect SiC formation which in our opinion had occurred in the presence of nickel acted as catalyst. It was our belief that SiC formation during DRM would have enhanced stability of catalyst activity and increased the possibility of sustainable production. This was also shown by time on stream analysis which had indicated only 5% loss in activity during reaction (Fig. 7).

Although TGA analysis showed no signs of coke formation, SEM images still revealed the presence of filamentous coke on catalyst surface. This could be a random case or the amount of coke formed during DRM could be miniscule. In any case, it would be better to obtain a third opinion about the presence of coke which could be achieved by Raman spectroscopy. Raman spectroscopy which was one of the most effective characterization methods to determine coke formation [43] indicated no carbon peak. Based on TGA and Raman spectroscopy it would be appropriate to state that the coke formed during DRM transformed into SiC and an undetectable amount of coke may have remained on catalyst surface.

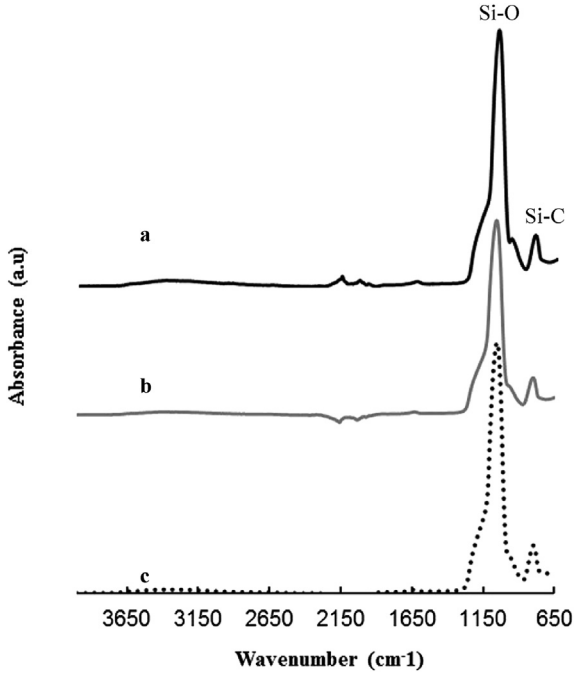

Fig. 10 – ATR-FT-IR analyses of (a) 1.25% Ni (b) 5% Ni (c) 10% Ni microsphere catalysts.

We have shown none or negligible coke formation during DRM. However we still need to validate a second analysis to validate the presence of SiC. The Attenuated total reflectance Fourier transform infrared spectroscopy (ATR-FT-IR) of the used catalysts was conducted for this purpose (Fig. 10). Results indicated the presence of two peaks around 1100–1200 cm^{-1} and 810–840 cm^{-1}, which belonged to Si–O and Si–C, respectively [44].

Conclusions

Ni/Si microsphere catalysts with high and stable activity has been synthesized and tested for DRM reaction. Results indicated that sustainable production of syngas with DRM reaction could have taken place with these catalysts. Activity loss in Nickel containing catalysts was generally emanated from coke formation and its deposition on catalyst surface. However, this had not been the case for our catalysts and characterization analyses conducted with spent catalysts revealed that none or negligible amount of coke had been deposited on catalyst surface during reaction. Since it was impossible to prevent methane cracking or Boudard reaction during DRM, a better explanation was needed for the disappearance of coke in the process. Interpretation of reaction experiments and characterization analyses of spent catalysts revealed formation of SiC which was reported for the first time based on our knowledge. SiC formation prevented the deposition of coke during DRM and enhanced the sustainability of catalytic activity. The negligible activity loss obtained during time on stream analysis also confirmed this conclusion.

Acknowledgements

Bilecik Seyh Edebali University Research Fund, BAP (2015-02.BŞEÜ.03-03) and contributions of Gazi University Kinetic Research Laboratory Group are gratefully acknowledged.

Abbreviations

DRM	Dry reforming of methane
SiC	Silicon carbide
RWGS	Reverse water gas shift reaction
SiO_2	Silica
CTAB	Hexadecyl cetyl trimethyl ammonium bromide
TEOS	Tetraethylorthosilicate
XRD	X-ray diffraction
SEM	Scanning electron microscopy

ICP-MS Inductively coupled plasma
TGA Thermal analysis
ATR-FT-IR Attenuated total reflectance Fourier transform infrared spectroscopy

Appendix A. Supplementary data

Supplementary data related to this article can be found at http://dx.doi.org/10.1016/j.ijhydene.2017.05.121.

REFERENCES

[1] Shang Z, Li S, Li L, Liu G, Liang X. Highly active and stable alumina supported nickel nanoparticle catalysts for dry reforming of methane. Appl Catal B Environ 2017;201:302–9.
[2] Wolfbeisser A, Sophiphun O, Bernardi J, Wittayakun J, Föttinger K, Rupprechter G. Methane dry reforming over ceria-zirconia supported Ni catalysts. Catal Today 2016;277(2):234–45. http://dx.doi.org/10.1016/j.cattod.2016.04.025.
[3] Singha KR, Yadav A, Agrawal A, Shukla A, Adak S, Sasaki T, et al. Synthesis of highly coke resistant Ni nanoparticles supported MgO/ZnO catalyst for reforming of methane with carbon dioxide. Appl Catal B Environ 2016;191:165–78.
[4] Titus J, Roussiere T, Wasserschaff G, Schunk S, Milanov A, Schwab E, et al. Dry reforming of methane with carbon dioxide over NiO-MgO-ZrO_2. Catal Today 2016;270:68–75.
[5] Wang F, Xu L, Shi W. Syngas production from CO_2 reforming with methane over core-shell Ni@SiO_2 catalysts. J CO_2 Util 2016;16:318–27.
[6] Bian Z, Suryawinata YI, Kawi S. Highly carbon resistant multicore-shell catalyst derived from Ni-Mg phyllosilicate nanotubes@silica for dry reforming of methane. Appl Catal B Environ 2016;195:1–8.
[7] Bao Z, Lu Y, Han J, Li Y, Yu F. Highly active and stable Ni-based bimodal pore catalyst for dry reforming of methane. Appl Catal A Gen 2015;491:116–26.
[8] Kang KM, Kim HW, Shim IIW, Kwak HY. Catalytic test of supported Ni catalysts with core/shell structure for dry reforming of methane. Fuel Process Technol 2011;92:1236–43.
[9] Zheng X, Tan S, Dong L, Li S, Chen H. $LaNiO_3$@SiO_2 core-shell nano-particles for the dry reforming of CH4 in the dielectric barrier discharge plasma. Int J Hydrogen Energy 2014;39:11360–7.
[10] Li D, Li R, Lu M, Lin X, Zhan Y, Jiang L. Carbon dioxide reforming of methane over Ru catalysts supported on Mg-Al oxides: a highly dispersed and stable Ru/Mg(Al)O catalyst. Appl Catal B Environ 2017;200:566–77.
[11] Kwak BS, Kim J, Kang M. Hydrogen production from ethanol steam reforming over core-shell structured NixOy-, FexOy-, and CoxOy-Pd catalysts. Int J Hydrogen Energy 2010;35:11829–43.
[12] Medeiros RLBA, Macedo HP, Melo VRM, Oliveira AAS, Barros JMF, Melo MAF, et al. Ni supported on Fe-doped $MgAl_2O_4$ for dry reforming of methane: use of factorial design to optimize H_2 yield. Int J Hydrogen Energy 2016;41:14047–57.
[13] Ali S, Almarri MJ, Abdelmoneim AG, Kumar A, Khader MM. Catalytic evaluation of nickel nanoparticles in methane steam reforming. Int J Hydrogen Energy 2016:1–10. http://dx.doi.org/10.1016/j.ijhydene.2016.08.200.
[14] Ayodele BV, Khan MR, Cheng CK. Catalytic performance of ceria-supported cobalt catalyst for CO-rich hydrogen production from dry reforming of methane. Int J Hydrogen Energy 2016;41:198–207.
[15] Yang EH, Noh YS, Ramesh S, Lim SS, Moon DJ. The effect of promoters in $La_{0.9}M_{0.1}Ni_{0.5}Fe_{0.5}O_3$ (M = Sr, Ca) perovskite catalysts on dry reforming of methane. Fuel Process Technol 2015;134:404–13.
[16] Benrabaa R, Löfberg A, Caballero JG, Richard EB, Rubbens A, Vannier RN, et al. Sol-gel synthesis and characterization of silica supported nickel ferrite catalysts for dry reforming of methane. Catal Commun 2015;58:127–31.
[17] Kaynar ADD, Dogu D, Yasyerli N. Hydrogen production and coke minimization through reforming of kerosene over bi metallic ceria-alumina supported Ru-Ni catalysts. Fuel Process Technol 2015;140:96–103.
[18] Zhang J, Li F. Coke-resistant Ni@SiO_2 catalyst for dry reforming of methane. Appl Catal B Environ 2015;176–177:513–21.
[19] Majewski AJ, Wood J, Bujalski W. Nickel-silica core@shell catalyst for methane reforming. Int J Hydrogen Energy 2013;38:14531–41.
[20] Jo SW, Kwak BS, Kim KM, Do JY, Park NK, Lee TJ, et al. Reasonable harmony of Ni and Mn in core@shell-structured NiMn@SiO_2 catalysts prepared for hydrogen production from ethanol steam reforming. Chem Eng J 2016;288:858–68.
[21] Ding C, Gao X, Han Y, Ma X, Wang J, Liu S, et al. Effects of surface states over core-shell Ni@SiO_2 catalysts on catalytic partial oxidation of methane to synthesis gas. J Energy Chem 2015;24:45–53.
[22] Meng SC, Wang H, Qing M, Qiu CW, Yang Y, Li YW. Preparation and characterization of SiO_2@Fe_2O_3 core-shell catalysts. J Fuel Chem Technol 2015;43:692–700.
[23] Yang W, Liu H, Li Y, Zhang J, Wu H, He D. Properties of yolk-shell structured Ni@SiO_2 nanocatalyst and its catalytic performance in carbon dioxide reforming of methane to syngas. Catal Today 2016;259:438–45.
[24] Wang Z, Hu X, Dong D, Parkinson G, Li CZ. Effects of calcination temperature of electrospun fibrous Ni/Al_2O_3 catalysts on dry reforming of methane. Fuel Process Technol 2016;155:246–51. http://dx.doi.org/10.1016/j.fubroc.2016.08.001.
[25] Kang D, Lee JW. Enhanced methane decomposition over nickel-carbon-B_2O_3 core-shell catalysts derived from carbon dioxide. Appl Catal B Environ 2016;186:41–55.
[26] Zhao X, Li H, Zhang J, Shi L, Zhang D. Design and synthesis of NiCe@m-SiO_2 yolk-shell framework catalysts with improved coke- and sintering-resistance in dry reforming of methane. Int J Hydrogen Energy 2016:1–10. http://dx.doi.org/10.1016/j.ijhydene.2015.10.111.
[27] Kang D, Lim HS, Lee JW. Enhanced catalytic activity of methane dry reforming by the confinement of Ni nanoparticles into mesoporous silica. Int J Hydrogen Energy 2017;42:11270–82.
[28] Omoregbe O, Danh HT, Nguyen-Huy C, Setiabudi HD, Abidin SZ, Truong QD, et al. Syngas production from methane dry reforming over Ni/SBA-15 catalyst: effect of operating parameters. Int J Hydrogen Energy 2017;42:11283–94.
[29] Zhang Q, Long K, Wang J, Zhang T, Song Z, Lin Q. A novel promoting effect of chelating ligand on the dispersion of Ni species over Ni/SBA-15 catalyst for dry reforming of methane. Int J Hydrogen Energy 2017;42(20):14103–14. http://dx.doi.org/10.1016/j.ijhydene.2017.04.090.
[30] Li B, Su W, Lin W, Wang X. Catalytic performance and characterization of Neodymium-containing mesoporous silica supported nickel catalysts for methane reforming to syngas. Int J Hydrogen Energy 2017;42(17):12197–209. http://dx.doi.org/10.1016/j.ijhydene.2017.03.159.
[31] Galvez ME, Albarazi A, Da Costa P. Enhanced catalytic stability through non-conventional synthesis of Ni/SBA-15

for methane dry reforming at low temperatures. Appl Catal A General 2015;504:143–50.
[32] Degirmenci L, Orbey N. Microencapsulation of silicotungstic acid to retain catalytic activity. Ind Eng Chem Res 2013;52:16714–8.
[33] Arbag H, Yasyerli S, Yasyerli N, Dogu G, Dogu T, Crnivec IGO, et al. Coke minimization during conversion of biogas to syngas by bimetallic tungsten-nickel incorporated mesoporous alumina synthesized by the one-pot route. Ind Eng Chem Res 2015;54:2290–301.
[34] Arbag H, Yasyerli S, Yasyerli N, Dogu G, Dogu T. Enhancement of catalytic performance of Ni based mesoporous alumina by Co incorporation in conversion of biogas to synthesis gas. Appl Catal B Environ 2016;198:254–65.
[35] Zhang S, Shi C, Chen B, Zhang Y, Qiu J. An activity and coke resistant dry reforming catalyst comprising nickel-tungsten alloy nanoparticles. Catal Commun 2015. http://dx.doi.org/10.1016/j.catcom.2015.06.003.
[36] Arbag H, Yasyerli S, Yasyerli N, Dogu G. Activity and stability enhancement of Ni-MCM 41 catalysts by Rh incorporation for hydrogen from dry reforming of methane. Int J Hydrogen Energy 2010;35:2296–304.
[37] Naumov S. Hysteresis phenomena in mesoporous materials [Ph.D. thesis]. Von der Fakultät für Physik und Geowissenschaften der Universität Leipzig; July 2009.
[38] Unutulmazsoy Y, Merkle R, Fischer D, Manhart J, Maier J. The oxidation kinetics of thin nickel films between 250 and 500 °C. Phys Chem Chem Phys 2017;19:9045–52.
[39] Haugsrud R. On the high-temperature oxidation of nickel. Corros Sci 2003;45:211–35.
[40] Kormanyos A, Endrödi B, Ondok R, Sapi A, Janaky C. Controlled photocatalytic synthesis of core-shell SiC/polyaniline hybrid nanostructures. Materials 2016. http://dx.doi.org/10.3390/ma9030201.
[41] Houyem A, Selmane EBHH. Silicon carbide: synthesis and properties, properties and applications of silicon carbide. http://dx.doi.org/10.5772/15736. https://www.intechopen.com/books/properties-and-applications-of-silicon-carbide/silicon-carbide-synthesis-and-properties [accessed 14.05.17.].
[42] Plumpton AJ. In: Production and processing of fine particles. Proceedings, vol. 7. Montreal: Pergamon Press; 1988. p. 581–8.
[43] Grodecki K, Jozwik I, Baranowski JM, Teklinska D, Strupinski W. SEM and Raman analysis of graphene on SiC (0001). Micron 2016;80:20–3.
[44] Vennekamp M, Bauer I, Groh M, Sperling E, Ueberlein S, Myndyk M, et al. Formation of SiC nanoparticles in an atmospheric microwave plasma. Beilstein J Nanotechnol 2011;2:665–73.